DALTON
FULL PAPER

Synthesis and characterization of Re^{V}, Re^{VI} and Re^{VII} complexes of the $[\alpha_2\text{-}P_2W_{17}O_{61}]^{10-}$ isomer †

Anne Venturelli,[a] Mark J. Nilges,[b] Alex Smirnov,[b] R. L. Belford[b] and Lynn C. Francesconi*[a]

[a] *Department of Chemistry, Hunter College of the City University of New York, New York, NY 10021, USA*
[b] *Illinois EPR Research Center, College of Medicine, University of Illinois-Champaign/Urbana, Urbana, IL 61801, USA*

Received 8th July 1998, Accepted 13th November 1998

Rhenium-(V), -(VI) and -(VII) complexes of the $[\alpha_2\text{-}P_2W_{17}O_{61}]^{10-}$ isomer, a mono-lacunary derivative of the $[\alpha\text{-}P_2W_{18}O_{62}]^{6-}$ (Wells–Dawson) ion have been prepared and characterized by multinuclear NMR spectroscopy, electrospray mass spectrometry and electron paramagnetic resonance spectroscopy, among other techniques. The molecules have the formulation $[\alpha_2\text{-}ReOP_2W_{17}O_{61}]^{n-}$, where n = 7,6,5 for Re^{V}, Re^{VI} and Re^{VII}, respectively. ^{183}W NMR spectroscopy for the Re^{V} and Re^{VII} analogs shows that the molecules have C_s symmetry, as expected for substitution in the α_2 site. Simulations of the X-band and Q-band EPR spectra of the Re^{VI} analog, using C_s symmetry, allow determination of the g, hyperfine and quadrupole coupling tensors. X-Band, Q-band and W-band EPR spectroscopy show extreme variations in linewidths due to random strains or distortions of the complex.

Introduction

The $[\alpha_2\text{-}P_2W_{17}O_{61}]^{10-}$ isomer, shown in Fig. 1, may be a useful ligand for stabilizing high valent transition and rare-earth (actinide and lanthanide) metal ions.[1] The $[\alpha_2\text{-}P_2W_{17}O_{61}]^{10-}$ isomer is obtained by base degradation of the parent Wells–Dawson molecule, $[\alpha\text{-}P_2W_{18}O_{62}]^{6-}$ (Fig. 1); effectively, removal of a $[WO]^{4+}$ unit from a "cap" WO_6 polyhedron of the parent $[\alpha\text{-}P_2W_{18}O_{62}]^{6-}$ results in the defect or lacunary structure of C_s symmetry.[1]

Well characterized, stable, complexants may find a number of applications in biochemistry and medicine, catalysis, as well as separation of high valent metal ions from waste streams. In the medicinal area, for example, a number of families of polyoxoanions, have been shown to interact with enzymes specifically, suggesting that these compounds may be valuable for study of the structure and function of enzymes and proteins.[2] Polyoxoanions, including derivatives of the $[\alpha_2\text{-}P_2W_{17}O_{61}]^{10-}$ isomer, have also been noted for anti-viral activity.

In the area of catalysis, while there are few reports of the catalytic properties of derivatives of the Wells–Dawson molecule, "Keggin" derivatives are well known thermal catalysts and, recently, photocatalysts, for oxidative transformation of various organic molecules in solution.[3,4] Derivatives of the Keggin and Wells–Dawson molecules appear to be stable under conditions found in catalytic reactions. A useful property of polyoxoanions is their resistance to decomposition by self-oxidation. Complexes can be rendered soluble in aqueous or organic solution by an appropriate choice of counter cation(s). Transition metal derivatives of isomerically pure $[\alpha_2\text{-}P_2W_{17}O_{61}]^{10-}$ have been subjected to oxidation catalysis studies.[5]

We are investigating the chemistry of nonoxidizable lacunary tungstate, $[\alpha_2\text{-}P_2W_{17}O_{61}]^{10-}$, with rare earth ions[6,7] and technetium and rhenium[8] for a variety of applications. While using rhenium as a "surrogate" for technetium,[9] we found that the chemistry of high oxidation state rhenium incorporated into the $[\alpha_2\text{-}P_2W_{17}O_{61}]^{10-}$ polyoxoanion framework is quite rich, similar to that found by Pope for Re incorporated into two other "cage" systems.[10,11] In that work, complexes of Re(V), Re(VI) and Re(VII) have been isolated for both the Keggin and $[W_{10}O_{32}]^{4-}$ families of compounds, establishing that high valent rhenium in oxidation states V, VI, VII, can be stabilized within polyoxoanion frameworks. We add to this database by providing, for the first time, multinuclear NMR data and electrospray mass spectrometry data for the structural characterization of Re complexes of $[\alpha_2\text{-}P_2W_{17}O_{61}]^{10-}$. The reaction of $ReCl_6^{2-}$ and $[\alpha_2\text{-}P_2W_{17}O_{61}]^{10-}$ has been reported by Charreton and Meunier,[12] however, neither a detailed procedure nor characterization of the material was presented. The details of the preparation, characterization and chemistry of Re(V), Re(VI) and Re(VII) complexes of the $[\alpha_2\text{-}P_2W_{17}O_{61}]^{10-}$ polyoxoanion constitute this report.

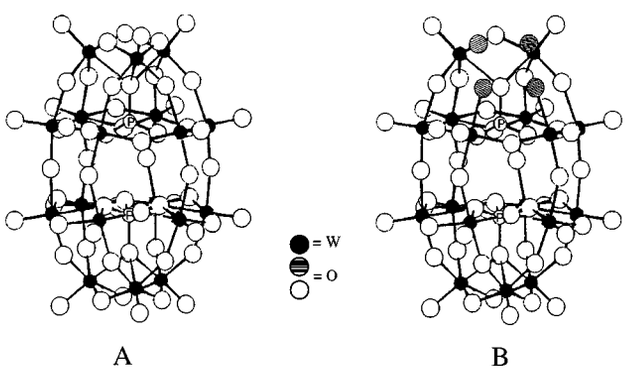

Fig. 1 Ball and stick model of A $[\alpha\text{-}P_2W_{18}O_{62}]^{6-}$ and B the lacunary $[\alpha_2\text{-}P_2W_{17}O_{61}]^{10-}$ ligand.

There have been other reports of the preparation of transition metal complexes of the $[\alpha_2\text{-}P_2W_{17}O_{61}]^{10-}$ isomer, where characterization has included multinuclear NMR techniques. For example, both ^{31}P and ^{183}W NMR spectroscopy provided proof that transition metal derivatives of mixtures of the α_2 and α_1 isomers of $[P_2W_{17}O_{61}]^{10-}$ can be prepared by base degradation of the parent $[\alpha/\beta\text{-}P_2W_{18}O_{62}]^{6-}$.[13] Isomerically pure $[\alpha_2\text{-}P_2W_{17}O_{61}]^{10-}$ was used to prepare a variety of transition metal

† *Supplementary data available*: cyclic voltammogram of **1**; ^{31}P NMR spectra of **1a**, **3** and **2**; ^{183}W NMR spectrum of **3**. Available from BLDSC (No. SUP 57462, 5 pp.) or the RSC Library. See Instructions for Authors, 1999, Issue 1 (http://www.rsc.org/dalton).

derivatives. These compounds, characterized by a variety of techniques, including both ^{31}P and ^{183}W NMR spectroscopy, constitute the first isolated monosubstituted Wells–Dawson complexes free of the α_1 isomer as an impurity.[14] In another study, 2-D ^{183}W NMR spectroscopy was used to completely assign all of the ^{183}W resonances and connectivities of the lacunary $[\alpha_2\text{-}P_2W_{17}O_{61}]^{10-}$ ligand and the $V^V{=}O$ (d^0) derivative, $[\alpha_2\text{-}VP_2W_{17}O_{62}]^{7-}$.[15]

High valent oxorhenium complexes and Re(VII) oxides have experienced interest for their unique redox properties and potential for oxidation catalysts.[16–19] There has been increasing interest in methylrhenium trioxide[20] as a potential epoxidation catalyst.

We report herein the preparation and isolation of Re complexes of the $[\alpha_2\text{-}P_2W_{17}O_{61}]^{10-}$ isomer and characterization, by multinuclear NMR spectroscopy, EPR spectroscopy, electrospray ionization mass spectrometry among other techniques. In this work, we use the early report by Charreton and Meunier[12] as a starting point to prepare the $K_7[\alpha_2\text{-}Re^VOP_2W_{17}O_{61}]$ species **1** in excellent yield. Oxidation of this species affords the Re^{VI} **2** and Re^{VII} **3** analogs.

Experimental

General comments

Most common laboratory chemicals were reagent grade, purchased from commercial sources and used without further purification. Deionized distilled water was used throughout. Preparative operations unless stated otherwise were carried out under atmospheric conditions. Standard Schlenk techniques under an atmosphere of nitrogen were also utilized. $K_{10}[\alpha_2\text{-}P_2W_{17}O_{61}]$ was prepared according to the method of Finke;[14,21] this is important to insure that the resulting rhenium complexes are isomerically pure. NBu_4Br (Fisher), AgO_3SCF_3 (Aldrich), and H_2SO_4 (Fisher) were purchased and used without further purification. Elemental analysis was performed by the University of Illinois Microanalytical Laboratory. Negative-ion electrospray mass spectra were recorded on a VG Quattro at the University of Illinois School of Chemical Sciences Mass Spectrometry Laboratory. Electrochemical analyses were accomplished with the use of a Bioanalytical Systems BAS-100 electrochemical analyzer.

Collection of NMR data

NMR spectra were obtained on a JEOL GX-400 spectrophotometer. ^{31}P NMR spectra at 161.8 MHz were acquired using a broad band decoupler coil of a 5 mm reverse detection probe. ^{183}W NMR spectra recorded at 16.7 MHz utilized a 10 mm low-frequency broad band probe. Typical acquisition parameters for ^{31}P spectra included the following: spectral width, 10,000 Hz; acquisition time, 0.8 s; pulse delay, 1.0 s; pulse width, 15 *v*s (50° tip angle). For ^{183}W spectra, typical conditions included the following: spectral width, 10,000 Hz; acquisition time, 1.6 s; pulse delay, 0.5 s; pulse width, 50 *v*s (45° tip angle). For all spectra, the temperature was controlled to ±0.2 °C. ^{31}P spectra were referenced to 85% H_3PO_4, and ^{183}W spectra were referenced to 2.0 M Na_2WO_4. For both ^{31}P and ^{183}W chemical shifts, the convention used is that the more negative chemical shifts denote upfield resonances.

Collection of EPR data

Electron paramagnetic resonance experiments were performed on Varian E-122 X-band (9.27 GHz), Varian E-15 Q-band (34.63 GHz), and the IERC Mark II W-band (94.43 GHz)[22] spectrometers. A microwave power of 2.0 mW was used with a modulation amplitude of 5.0 G for X-band and 10.0 G for Q- and W-band at 100 kHz. Samples were run at 77 K (at X- or Q-band) and 20 K (at W-band) as glasses of 0.01 M 50:50 acetonitrile–toluene solutions. The magnetic field was calibrated with a Varian NMR Gauss meter (X-band) and a Metrolab Teslameter (Q-band and W-band), and the microwave frequency was determined with an EIP frequency meter with extended frequency option (to 100 GHz). Because of the very large magnetic field scans used, X-band and Q-band field scans were corrected using a second and third order, respectively, least squares fit of the field calibration data with a resulting rms field error of 0.4 and 2.1 G, respectively.

Simulation and fitting of electron paramagnetic resonance spectra used the automated simulation program SIMPIP,[23] which is based upon QPOW.[24] The spin Hamiltonian is solved by exact diagonalization, followed by a fourth-order field-frequency perturbation to transform the energy spectrum into a field-swept spectrum. The spin Hamiltonian parameters are varied using the SIMPLEX method to minimize the rms deviation between the experimental and calculated spectrum.[25] Because of the large nonlinear effects in rhenium spectra due to the large hyperfine and nuclear quadrupole interaction, the "forbidden," $\Delta M_I = \pm1, \pm2, \pm3, \pm4$ and ±5 transitions were all included.

$$H = \{\beta B\cdot g\cdot S - \beta_n g_n B\cdot I\} + hS\cdot A\cdot I + hI\cdot P\cdot I$$

where g is the electronic Zeeman matrix, g_n is the nuclear Zeeman g-factor, A is the hyperfine matrix, P is the nuclear quadrupole coupling tensor, B and β_n are the Bohr and nuclear magnetons, respectively, and S and I are the electron and nuclear spin operators, respectively.

For this rhenium system, the linewidth is nearly completely dominated by strain effects, and simple M_I and M_I^2 dependant linewidth expressions are deemed inappropriate for spectra which are clearly not first-order. Strain effects were included by calculating exact analytical gradients of the eigenvalues of the spin Hamiltonian transformed to the field domain through the fourth-order frequency perturbation.

Rhenium has two naturally occurring isotopes ^{187}Re (62.6%) and ^{185}Re (37.4%). Because the ratio of moments is 0.9899:1, no splitting due to the isotopes is resolved, but in order to properly evaluate hyperfine and quadrupole strain effects, we had to include the spectra of both isotopes explicitly in the simulations.

Preparation of compounds

$K_7[\alpha_2\text{-}Re^VOP_2W_{17}O_{61}]$ 1. A 150 mL round-bottom flask was charged with K_2ReCl_6 (0.839g, 1.76 mmol), $K_{10}[\alpha_2\text{-}P_2W_{17}O_{61}]$ (6.67g, 1.47 mmol), and 80 mL of deionized H_2O resulting in a bright blue slurry. This mixture was refluxed for 30 minutes during which time the color of the solution became a dark purple-black color. The solvent was removed by rotary evaporation at 50 °C. To remove any impurities, the sample was dissolved in a minimum amount of hot H_2O (80 °C) (≈9 mL) and placed in a refrigerator to precipitate the product. The purple-brown solid was filtered off through a medium glass frit, and washed with 3 × 20 mL of EtOH followed by 3 × 30 mL of diethyl ether, to give 6.13 g of **1** (M of anion = 4635) in 90% yield. In order to increase solubility for ^{183}W NMR, the potassium salt was partially lithiated by a metathesis reaction wherein a stoichiometric amount of $LiClO_4$ was added to an aqueous solution of **1** precipitating $KClO_4$. ^{31}P NMR (D_2O): δ −11.86 (s), −12.86 (s). ^{183}W NMR (D_2O): δ −134 (s, 2W), −161 (s, 1W), −182 (s, 2W), −191 (s, 2W), −210 (s, 2W), −271 (s, 2W), −273 (s, 2W), −280 (s, 2W), −479 (s, 2W). Negative ESI-MS: ($[ReP_2W_{17}O_{62}]^{7-}$ = 4365) 872 (*m*/5), 1091 (*m*/4) (Calc. for $K_7O_{62}P_2ReW_{17}{\cdot}2\,H_2O$: K, 5.58; Cl, 0.0; P, 1.26; Re, 3.79; W, 63.67. Found: K, 5.15; Cl, 0.04; P, 1.16; Re, 4.02; W, 59.43%). Infrared (KBr, cm^{-1}): 1612.8s, 1090.9s, 1019.2 (sh), 953.5s, 905.2s, 777.4s (br), 597.4w, 564.1w, 523.1m.

$[NBu_4]_xK_{7-x}[\alpha_2\text{-}Re^{V}OP_2W_{17}O_{61}]$ 1a. A 50 mL Schlenk flask was charged with 5 mL of deoxygenated water and 0.100 g (0.022 mmol) of $K_7[\alpha_2\text{-}Re^{V}OP_2W_{17}O_{61}]$. To this brown solution was added 0.069 g (0.216 mmol) of solid NBu_4Br under a flow of N_2. The pH was maintained between 4 and 5 by the addition of 0.18 M H_2SO_4. After stirring for a few minutes, the solvent was removed *in vacuo* resulting in a brown solid. ^{31}P NMR (CD_3CN): δ −12.26 (s), −13.19 (s), and −12.70 (small amount of $[NBu_4]_6[P_2W_{18}O_{62}]$ impurity). The sample is air sensitive.

$[NBu_4]_6[\alpha_2\text{-}Re^{VI}OP_2W_{17}O_{61}]$ 2. In air, a solution of $K_7[\alpha_2\text{-}ReOP_2W_{17}O_{61}]$ (0.500 g, 0.107 mmol) in 100 mL of deionized water (initial pH 3.7) was treated with small portions of NBu_4Br (0.347 g, 1.07 mmol). The pH was maintained between 4 and 5 *via* the addition of 0.18 M H_2SO_4. This results in the formation of a brown solid which was filtered, and washed with 3 × 30 mL of water followed by 3 × 30 mL of diethyl ether. As the solid was drying under vacuum in the glass frit, the color of the solid changed from dark brown to a blue-green (over the course of two hours). Yield: 0.464 g (78%) (Calc. for $C_{96}H_{216}N_6O_{62}P_2ReW_{17}$: C, 19.81; H, 3.74; N, 1.44; P, 1.06; Re, 3.20; W, 53.70. Found: C, 20.35; H, 3.93; N, 1.30; P, 0.68; Re, 3.30; W, 53.64%). ^{31}P NMR (CD_3CN): δ −7.60 (br, s), −12.39 (s). Negative ESI-MS: 2^- charge state: $[NBu_4]_4[\alpha_2\text{-}Re^{VI}OP_2W_{17}O_{61}]$: 2666.9 $[NBu_4]_3H^+[\alpha_2\text{-}Re^{VI}OP_2W_{17}O_{61}]$: 2546.4; 3^- charge state: $[NBu_4]_3[\alpha_2\text{-}Re^{VI}OP_2W_{17}O_{61}]$: 1697.3, $(NBu_4)_2H^+[\alpha_2\text{-}Re^{VI}OP_2W_{17}O_{61}]$: 1616.9; 4^- charge state: $[NBu_4]H^+[\alpha_2\text{-}Re^{VI}OP_2W_{17}O_{61}]$: 1152.2; $2\ H^+[\alpha_2\text{-}Re^{VI}OP_2W_{17}O_{61}]$: 1091.9: 5^- charge state: $H+[\alpha_2\text{-}Re^{VI}OP_2W_{17}O_{61}]$: 873.3.

$[NBu_4]_5[\alpha_2\text{-}Re^{VII}OP_2W_{17}O_{61}]$ 3. To a 100 mL Schlenk flask charged with AgO_3SCF_3 (0.047 g, 0.18 mmol) and 5 mL of deoxygenated acetonitrile was added a deep green solution of $[NBu_4]_6[\alpha_2\text{-}Re^{VI}OP_2W_{17}O_{61}]$ in 20 mL of CH_3CN by cannula filtration. This results in a green solution with a gray solid (Ag^0). After stirring for two hours, the mixture was exposed to air and filtered through a nylon disk filter to remove the elemental silver. The solvent was removed by rotary evaporation leaving a pale green solid. The sample was redissolved in 2 mL of hot CH_3CN and filtered to remove any insoluble species. With stirring, *ca.* 4 mL of diethyl ether was added dropwise to precipitate a pale yellow solid. The solid was collected on a glass frit, and washed with 3 × 30 mL of ether to give 0.606 g of **3** (74%). ^{31}P NMR (CD_3CN): δ −11.70 (s), −13.33 (s). ^{183}W NMR (CD_3CN): δ −85.60 (1), −114.56 (2), −127.78 (2), −130.42 (2), −146.57 (2), −147.94 (2), −154.38 (2), −157.80 (2), −195.91 (2) (Calc. for $C_{80}H_{180}N_5O_{62}P_2ReW_{17}$: C, 17.23; H, 3.25; N, 1.26; P, 1.11; Re, 3.34; W, 56.04. Found: C, 17.09; H, 3.38; N, 1.09; P, 1.11; Re, 3.24; W, 56.65).

Results and discussion

Synthesis of complexes

$K_7[\alpha_2\text{-}ReOP_2W_{17}O_{61}]$. The reaction of an aqueous solution of K_2ReCl_6 and $K_{10}[\alpha_2\text{-}P_2W_{17}O_{61}]$ gives the purple-brown compound, $K_7[\alpha_2\text{-}ReOP_2W_{17}O_{61}]$ in 90% yield. This product was purified by recrystallization from hot H_2O. This reaction was reported in 1974, but no procedure or characterization of the product was provided.[12] We had attempted to prepare Re(v) complexes of $[\alpha_2\text{-}P_2W_{17}O_{61}]^{10-}$ using Re^{V} starting materials; however, our efforts resulted in mixtures of unidentifiable products, presumably a mixture of Re oxidation states. The reaction of the Re^{IV} reagent produces the desired product in excellent yield. Occasionally, in preparations of this compound, we observed a peak in the ^{31}P NMR spectrum at *ca.* δ +0.2 (<2%), signalling another species, perhaps a paramagnetic Re(VI) species. This impurity could be removed by recrystallization.

All of the data given below (elemental analysis, ^{31}P and ^{183}W NMR spectroscopy) and lack of EPR signal (X-Band, 9.5 GHz) over a wide magnetic range in the solid state (293 K) or a frozen water–ethylene glycol mixture (77 K), are consistent with a diamagnetic Re^{V}=O product. Apparently, the rhenium abstracts an oxo ligand from either the aqueous media or the lacunary tungstate cluster.

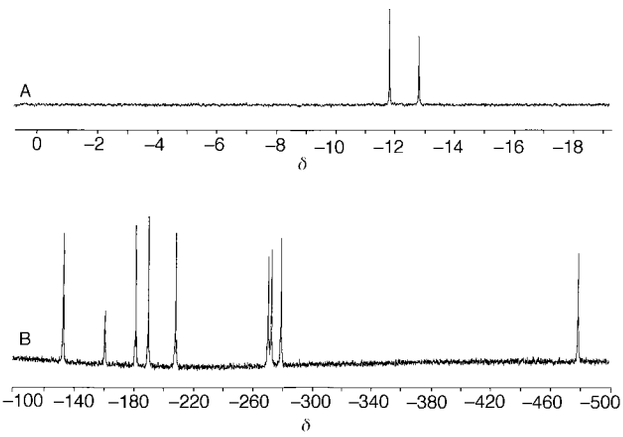

Fig. 2 A ^{31}P NMR spectrum of $K_7[\alpha_2\text{-}Re^{V}OP_2W_{17}O_{61}]$ **1** taken in D_2O, 20 mM. B ^{183}W NMR spectrum of $Li_xK_{7-x}[\alpha_2\text{-}Re^{V}OP_2W_{17}O_{61}]$, 0.2 M.

Elemental analysis clearly shows that there are no chloride atoms present and gives a reasonable analysis for $K_7O_{62}P_2ReW_{17}$. We and others have found that elemental analysis is often unreliable for analysis of polyoxoanions, especially for the tungsten analysis.[14] We find that other techniques, including multinuclear NMR spectroscopy are often more sensitive and accurate. The infrared spectrum, not surprisingly, is similar to the parent $P_2W_{18}O_{62}^{6-}$ species. In the previous study reported by Pope[10] the IR spectra of the Re^{V}, Re^{VI}, and Re^{VII} substituted lacunary $[XW_{11}O_{39}]^{n-}$ (X = Re^{V}, Re^{VI}, Re^{VII}) anion were indistinguishable from those of the corresponding $[XW_{12}O_{40}]^{n-}$ species.

A similar oxidation process has been reported in the reaction of $Ru^{III}Cl_3\cdot xH_2O$ with $[\alpha_2\text{-}P_2W_{17}O_{61}]^{10-}$ to give $[O\{Ru^{IV}Cl(\alpha_2\text{-}P_2W_{17}O_{61})\}_2]$.[26] We and others have found that the $[\alpha_2\text{-}P_2W_{17}O_{61}]$ framework is oxophilic, stabilizing ions with high charge : size ratio[27] such as tetravalent Ce.[28] In addition, preliminary reports in the Russian literature show stabilization of the quadrivalent oxidation state in transuranic (TRU) ions, like Am and Cf, by complexation with the lacunary heteropolyanion $[P_2W_{17}O_{61}]^{10-}$ in aqueous solutions.[29] In that context the oxidation of Re^{IV} to Re^{V} in this reaction is not surprising. The oxidation of Re^{IV} complexes upon incorporation into polyoxoanion frameworks may be an appropriate synthetic method to prepare rhenium complexes of other metal oxides.

We used isomerically pure $[\alpha_2\text{-}P_2W_{17}O_{61}]^{10-}$ as the starting material in this preparation. This is important as the preparation of metal complexes using base degradation of the parent $[\alpha_2\text{-}P_2W_{17}O_{61}]^{10-}$ isomer often results in mixtures of the α_2- and $\alpha_1\text{-}[P_2W_{17}O_{61}]^{10-}$ isomers.[13,14] Examination of the ^{31}P and ^{183}W NMR data, given below, are consistent with the production of isomerically pure $K_7[\alpha_2\text{-}ReOP_2W_{17}O_{61}]$.

The ^{31}P NMR spectrum of a D_2O solution of the Re(v) product, $K_7[\alpha_2\text{-}ReOP_2W_{17}O_{61}]$, consists of two sharp singlets at P(1) δ −11.86 and P(2) δ −12.86 indicative of two inequivalent phosphorus centers (Fig. 2A). P(1) is the phosphorous atom closest to the site of substitution. P(2) is that remote from the subsitution site. These resonances are different from the lacunary $K_{10}[\alpha_2\text{-}P_2W_{17}O_{61}]$ and further, the NMR indicates that the complex is >99% isomerically pure. For comparison, the positions of the two resonances in the parent $[\alpha_2\text{-}P_2W_{17}O_{61}]^{10-}$ and diamagnetic lanthanide complexes in water are at δ 7–8 for P(1) and at *ca.* 14 for P(2). There is a paucity of literature comparing the ^{31}P resonances of transition metal complexes incorporated into the $[\alpha_2\text{-}P_2W_{17}O_{61}]^{10-}$ framework, especially second or third

row metal ions. In one study, the $[\alpha_2\text{-}MoP_2W_{17}O_{62}]^{6-}$ species showed chemical shifts in water of δ −11.9 and −12.6, close to our complex.[30] The ^{31}P NMR spectrum of the paramagnetic Ru(IV) dimeric species, discussed above, identifies the broad resonance at δ +0.2 as the P(1) resonance and the P(2) resonance that at δ −13.2.[26]

Complexation of a ReO unit to the lacunary $K_{10}[\alpha_2\text{-}P_2W_{17}O_{61}]$ generates a plane of symmetry (C_s) through the molecule. The ^{183}W NMR spectrum of the partially lithiated $Li_xK_{7-x}[\alpha_2\text{-}ReOP_2W_{17}O_{61}]$ (0.2 M) in D_2O shows the expected nine line pattern, in which eight peaks integrate to two and one resonance integrates to one, and is assigned to the unique tungsten (Fig. 2B). The tungsten resonance shifted upfield, δ −479, is out of the range we usually observe for diamagnetic transition metal or lanthanide complexes of the $[\alpha_2\text{-}P_2W_{17}O_{61}]^{10-}$ isomer.[6,7] The two tungsten atoms represented by this resonance are shielded relative to the other tungsten atoms. This shielding may result from strong magnetic anisotropy of the Re=O bond. This resonance may be tentatively assigned to the two tungsten atoms in the "cap" region, connected to the Re=O unit *via* "edge bonding", each to two oxygen atoms in the cap. In other studies, of $[Re^{V}{=}O]^{3+}$ complexes of organic ligands, we have observed unusual upfield shifts for protons bound to carbon atoms in close proximity to the $[Re^{V}{=}O]^{3+}$ (or $[Tc^{V}{=}O]^{3+}$) site.[31]

Cyclic voltammetric studies on aqueous solutions of $K_7[\alpha_2\text{-}ReOP_2W_{17}O_{61}]$ (0.5 M LiO_2CCH_3, pH 4.7) reveal four redox waves with chemical potentials at +823, +476, −51, and −194 mV (platinum working electrode, Ag–AgCl reference electrode, Pt wire auxiliary electrode) (see SUP 57462, S1). The chemical potentials are assigned to Re^{7+}/Re^{6+} (+823 mV), Re^{6+}/Re^{5+} (+476 mV), and Re^{5+}/Re^{4+} (−51 mV). It is difficult to definitively assign the electrochemical potential located at −194 mV, this potential can be assigned to either the Re^{4+}/Re^{3+} couple or a reduction at the tungsten sites. The i_a/i_c ratios of non-unity and the ΔE_{pp} chemical potential separations of over 56 mV (ranging from 70–120 mV) over scan rates of 50 mV s^{-1} to 500 mV s^{-1} suggest electrochemical irreversibility.

We intend to study the aqueous electrochemistry of **1** at variable pH. The aqueous electrochemistry of both $[W_9Re^{V}O_{32}]^{5-}$ and $[SiW_{11}Re^{V}O_{40}]^{5-}$ show significant dependence on pH.[10,11] In those studies, reduction peaks assigned to the $Re^{5/4}$ and $Re^{4/3}$ couples were highly pH dependent. For both compounds, two one electron reductions were observed from pH 6 to pH 4 and one two electron process was observed below pH 4.

$[NBu_4]_xK_{7-x}[\alpha_2\text{-}Re^{V}OP_2W_{17}O_{61}]$ 1a. The oxidative conversion of $[NBu_4]_xK_{7-x}[\alpha_2\text{-}Re^{V}OP_2W_{17}O_{61}]$ to its Re^{6+} **2** analog can be prevented by treating an aqueous solution of $K_7[\alpha_2\text{-}Re^{V}OP_2W_{17}O_{61}]$ with NBu_4Br under strict anaerobic conditions. This reaction results in the formation of an aqueous-insoluble brown solid. SUP 57462, S2 shows the comparison of the ^{31}P NMR spectra of the tetrabutylammonium salts of the Re^{V}, Re^{VI}, and Re^{VII} complexes of $[\alpha_2\text{-}ReOP_2W_{17}O_{61}]^{n-}$. The chemical shift values are in line with those observed by Lyon for the tetrabutylammonium salts of a variety of transition metal derivatives of $[\alpha_2\text{-}P_2W_{17}O_{61}]^{10-}$ taken in CH_3CN–CD_3CN.[14] A small percentage of $[P_2W_{18}O_{62}]^{6-}$ (δ −12.70), is often observed as an impurity. The ^{31}P NMR spectrum of an acetonitrile solution of the NBu_4^+ salt of **1** consists of two phosphorus chemical shifts at δ −12.26 and −13.19 (SUP 57462, S2C).

$[NBu_4]_6[\alpha_2\text{-}Re^{VI}OP_2W_{17}O_{61}]$ 2. Performing the metathesis reaction of $K_7[\alpha_2\text{-}Re^{V}OP_2W_{17}O_{61}]$ in air, with NBu_4Br resulted in an oxidation of the Re(V) to Re(VI). Treatment of an aqueous solution of $K_7[\alpha_2\text{-}Re^{V}OP_2W_{17}O_{61}]$ with NBu_4Br, while maintaining the pH at 4–5, results in the formation of an aqueous-insoluble brown solid. As the brown solid dried under vacuum in a glass frit, the solid's color changed to blue-green. The molecule is paramagnetic; EPR data will be discussed later. A similar process in which a metathesis reaction resulted in oxidation was demonstrated recently by Pope in which conversion of $[CN_3H_6]_5[W_9Re^{V}O_{32}]$ to the NBu_4^+ salt resulted in an aerial oxidation of Re^{V} to Re^{VI}.[11] The ^{31}P NMR spectrum of a CD_3CN solution of $[NBu_4]_6[\alpha_2\text{-}Re^{VI}OP_2W_{17}O_{61}]$ **2** shows a broad peak at δ −7.60, due to the paramagnetism of the Re(VI) (d_1), and a sharp resonance at δ −12.39 (SUP 57462, S2B). Cyclic voltammetry of an acetonitrile solution of this blue complex showed four reversible redox features (glassy carbon working electrode, Pt auxiliary electrode, Ag–AgCl reference electrode, 0.1 M NBu_4PF_6) at +261 (Re^{VII}/Re^{VI}), −292 (Re^{VI}/Re^{V}), −1151 (Re^{V}/Re^{IV}), and −1363 mV (Re^{IV}/Re^{III} or tungsten reduction) (Fig. 3). The reduction processes were reversible over scan rates of 50 mV s^{-1} to 450 mV s^{-1}. Electrochemical studies of $[Re^{V}OPW_{11}O_{39}]^{4-}$ showed four oxidative/reductive processes which were assigned to rhenium in oxidation states ranging from III to VII.[9] The technetium analog, $[Tc^{V}OPW_{11}O_{39}]^{4-}$ however, showed a single reversible oxidation and a quasireversible reduction.[32]

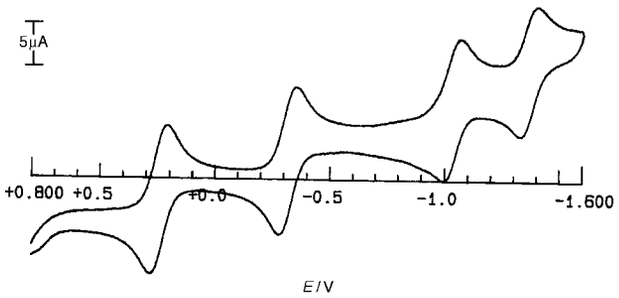

Fig. 3 Cyclic voltammogram of $[NBu_4]_6[\alpha_2\text{-}Re^{VI}OP_2W_{17}O_{61}]$ **2** taken in CD_3CN (glassy carbon working electrode, Pt auxiliary electrode, Ag–AgCl reference electrode, 0.1 M NBu_4PF_6), 100 mV s^{-1}.

$[NBu_4]_5[\alpha_2\text{-}Re^{VII}OP_2W_{17}O_{61}]$ 3. Treatment of a green acetonitrile solution of $[NBu_4]_6[\alpha_2\text{-}Re^{VI}OP_2W_{17}O_{61}]$ with an excess of AgO_3SCF_3 (1.2 equivalents) leads to the oxidation of the Re from +6 to +7, and a solution color change from deep green to a pale yellow-green. The ^{31}P NMR spectrum of this species consists of two sharp singlets at δ −11.70 and −13.33 (SUP 57462, 52A). Elemental analysis of this yellow solid confirms the formulation of $[NBu_4]_5[\alpha_2\text{-}Re^{VII}OP_2W_{17}O_{61}]$ ($C_{80}H_{180}N_5O_{62}P_2ReW_{17}$). Electrochemical studies of this highly oxidized species show the same CV as seen for the Re(VI) complex. These data are consistent with the complexes having the same structure.

The ^{183}W NMR spectrum of $[NBu_4]_5[\alpha_2\text{-}Re^{VII}OP_2W_{17}O_{61}]$ (SUP 57462, S3) also showed nine resonances, eight integrating for two and one integrating for one. This pattern confirms a molecule of C_s symmetry as would be found by substitution in the "cap" position of the $[\alpha_2\text{-}P_2W_{17}O_{61}]^{10-}$ isomer. The resonances for this species are different from the lacunary species, the Re^{V} species are within the range usually observed for diamagnetic metal complexes of the $[\alpha_2\text{-}P_2W_{17}O_{61}]^{10-}$ isomer.

Electrospray mass spectrometry

Fast-atom bombardment mass spectrometry of $K_7[\alpha_2\text{-}ReOP_2W_{17}O_{61}]$ was uninformative due to substantial cluster fragmentation. We found that negative-ion electrospray mass spectrometry provided data with minimal fragmentation. Electrospray ionization is a softer ionization technique than FAB, therefore it is commonly used for large and/or labile proteins and polymers.[33] Other electrospray ionization mass spectral analyses conducted on molybdenum and tungsten, "cage" compounds of the Lindquist, Keggin, octamolybdate and decatungstate structures, showed the polyoxoanions as base peaks with minimal degree of fragmentation in organic,

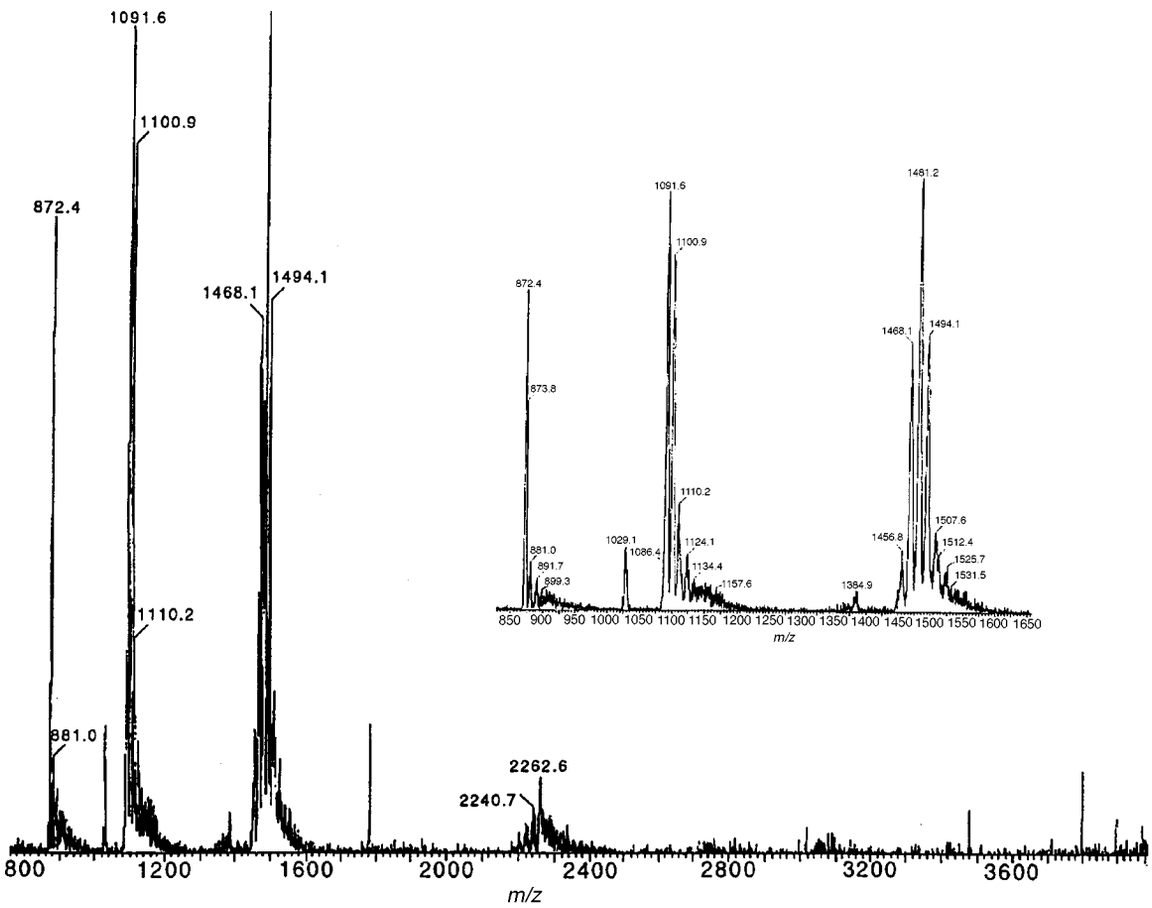

Fig. 4 Electrospray mass spectrum of $K_7[\alpha_2\text{-}Re^{V}OP_2W_{17}O_{61}]$ **1**. Inset shows expansion of m/z = 850 to 1650 region.

aqueous organic and aqueous solutions.[34a,b] One study displayed the potential for ES-MS to monitor equilibrium processes of aqueous polyoxoanion mixtures with time.[34b]

Polyoxoanions are highly negatively charged molecules and form adducts with cations, such as K^+ and H^+, in this case. Thus, different charge states can be formed. The ES mass spectrum for $K_7[\alpha_2\text{-}ReOP_2W_{17}O_{61}]$, taken in water, displayed in Fig. 4, shows the 2−, 3−, 4− and 5− charge regions. The inset shows an expansion of the 3−, 4− and 5− charge regions. Fig. 4 and Table 1 show the corresponding m/z values for the various charge states of the molecule with variable amounts of potassium and proton adducts. The electrospray mass spectrum for $[NBu_4]_6[\alpha_2\text{-}Re^{VI}OP_2W_{17}O_{61}]$ species, taken in acetonitrile, also is consistent with the theoretical values for the 2−, 3−, 4− and 5− charge states, with variable amounts of tetrabutylammonium cations adducts. One must be cautious, however, as the electrospray mass spectral technique may not distinguish oxoanions of different Re oxidation states well. In these cases, the oxoanions may differ by only one proton adduct and thus, would have the same or close to the same m/z value.

EPR studies of $[NBu_4]_6[\alpha_2\text{-}Re^{VI}OP_2W_{17}O_{61}]$

X-Band, Q-band and W-band EPR spectra shown in Fig. 5, 6 and 7, S4, respectively, show remarkable changes, especially in linewidth. For the X-band spectrum, Fig. 5, the linewidth varies from 25 G at lowest fields to more than 120 G at highest fields. In the Q-band spectrum, Fig. 6, the linewidth varies from 80 to 280 G, and in the W-band spectrum, Fig. 7, the linewidth varies from 250 to 700 G. This linewidth variation can be readily ascribed to random strains or distortions of the rhenium ion complex with a resultant distribution of spin Hamiltonian parameters, particulary in the g-tensor. The values of the g-, A- and P- tensors can be found in Table 2 and comparative

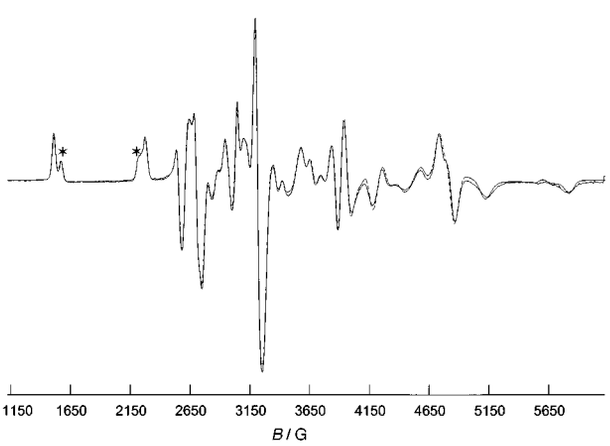

Fig. 5 X-Band (9.27 GHz) electron paramagnetic resonance spectrum of $[NBu_4]_6[\alpha_2\text{-}Re^{VI}OP_2W_{17}O_{61}]$ **2** in a CH_3CN–C_7H_8 glass at 77 K. Experimental (——), simulated (– – –). The asterisks mark forbidden M_I = 5/3 to 3/2 and M_I = 3/2 to 5/2 transitions. See text.

EPR parameters for d^1 systems in heteropolytungstates can be found in Table 3.

While some of the perpendicular (or 'z') features can be readily assigned in the spectra at all three frequencies, the perpendicular (or 'x' and 'y') features are poorly resolved at the higher frequencies. The "perpendicular" X-band cannot be assigned to any first-order splitting pattern, and analysis of the X-band spectrum shows that putatively "forbidden" $\Delta M_I = \pm 1, \pm 2, \ldots$ transitions completely dominate this part of the spectrum and that they have become "allowed" while the putatively "allowed" $\Delta M_I = 0$ transitions have become "forbidden." The observation of such strong forbidden transitions can be ascribed to state-mixing of the nuclear and electronic levels, the

Table 1 Electrospray mass spectral data for $K_7[ReO(\alpha_2\text{-}P_2W_{17}O_{61})]$ **1**[a] and $[N(Bu)_4]_6[ReO(\alpha_2\text{-}P_2W_{17}O_{61})]$ **2**[b]

$K_7[Re^{V}O(\alpha_2\text{-}P_2W_{17}O_{61})]$

Charge state	Species	*m*/*z*
2−	$K_5[ReO(\alpha_2\text{-}P_2W_{17}O_{61})]^{2-}$	2280.3
2−	$K_4H[ReO(\alpha_2\text{-}P_2W_{17}O_{61})]^{2-}$	2261.2
2−	$K_3H_2[ReO(\alpha_2\text{-}P_2W_{17}O_{61})]^{2-}$	2242.2
2−	$K_2H_3[ReO(\alpha_2\text{-}P_2W_{17}O_{61})]^{2-}$	2223.1
2−	$KH_4[ReO(\alpha_2\text{-}P_2W_{17}O_{61})]^{2-}$	2204.1
3−	$K_4[ReO(\alpha_2\text{-}P_2W_{17}O_{61})]^{3-}$	1507.1
3−	$K_3H[ReO(\alpha_2\text{-}P_2W_{17}O_{61})]^{3-}$	1494.3
3−	$K_2H_2[ReO(\alpha_2\text{-}P_2W_{17}O_{61})]^{3-}$	1481.7
3−	$KH_3[ReO(\alpha_2\text{-}P_2W_{17}O_{61})]^{3-}$	1469.0
3−	$H_4[ReO(\alpha_2\text{-}P_2W_{17}O_{61})]^{3-}$	1456.3
4−	$K_3[ReO(\alpha_2\text{-}P_2W_{17}O_{61})]^{4-}$	1120.6
4−	$K_2H[ReO(\alpha_2\text{-}P_2W_{17}O_{61})]^{4-}$	1111.1
4−	$KH_2[ReO(\alpha_2\text{-}P_2W_{17}O_{61})]^{4-}$	1101.5
4−	$H_3[ReO(\alpha_2\text{-}P_2W_{17}O_{61})]^{4-}$	1092.0
5−	$K_2[ReO(\alpha_2\text{-}P_2W_{17}O_{61})]^{5-}$	888.6
5−	$KH[ReO(\alpha_2\text{-}P_2W_{17}O_{61})]^{5-}$	881.0
5−	$H_2[ReO(\alpha_2\text{-}P_2W_{17}O_{61})]^{5-}$	873.4

$[NBu_4]_6[Re^{VI}O(\alpha_2\text{-}P_2W_{17}O_{61})]$

Charge state	Species	*m*/*z*
2−	$[NBu_4]_4[ReO(\alpha_2\text{-}P_2W_{17}O_{61})]^{2-}$	2666.9
2−	$[NBu_4]_3H[ReO(\alpha_2\text{-}P_2W_{17}O_{61})]^{2-}$	2546.1
3−	$[NBu_4]_3[ReO(\alpha_2\text{-}P_2W_{17}O_{61})]^{3-}$	1697.3
3−	$[NBu_4]_2H[ReO(\alpha_2\text{-}P_2W_{17}O_{61})]^{3-}$	1616.9
4−	$[NBu_4]_2H[ReO(\alpha_2\text{-}P_2W_{17}O_{61})]^{4-}$	1152.2
4−	$H_2[ReO(\alpha_2\text{-}P_2W_{17}O_{61})]^{4-}$	1091.9
5−	$H[ReO(\alpha_2\text{-}P_2W_{17}O_{61})]^{5-}$	873.3

[a] $[Re^{V}{=}O(\alpha_2\text{-}P_2W_{17}O_{61})]^{7-}$ $M = 4365$, sample dissolved in water. [b] $[Re^{VI}{=}O(\alpha_2\text{-}P_2W_{17}O_{61})]^{6-}$ $M = 4365$, sample dissolved in acetonitrile.

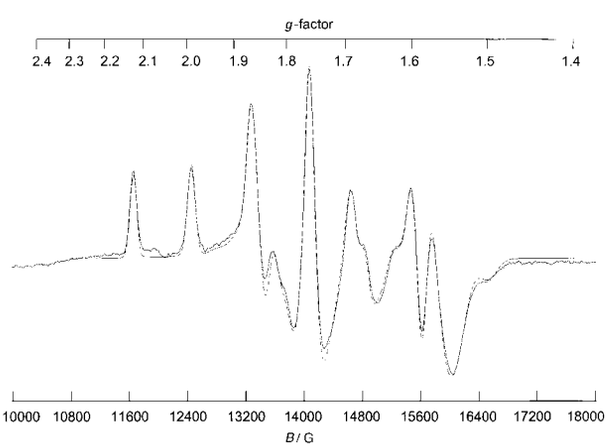

Fig. 6 Q-Band (34.63 GHz) electron paramagnetic resonance spectrum of $[NBu_4][\alpha_2\text{-}Re^{VI}OP_2W_{17}O_{61}]$ **2** in a CH_3CN–C_7H_8 glass at 77 K. Experimental (——), simulated (– – –).

splittings of which are of comparable strength at X-band. The two lowest field transitions of the "parallel" part of the X-band spectrum, which can be assigned to allowed $M_I = 5/2$ and 3/2 transitions appear to be split (Fig. 5). These extra peaks, marked with asterisks, are actually "forbidden" $m_I = 5/2$ to 3/2 and $m_I = 3/2$ to 5/2 transitions. The spacing between these two peaks is equal in first-order to $8QD/g_{eff}\beta$, where $QD{=}3/2P_z$. From this splitting we obtain $QD = 203$ MHz, which compares well with the value of 209 MHz obtained with spectral simulation, Table 3. This is one of the best examples to date of how state-mixing can allow the direct measurement of the nuclear quadrupole coupling from a powder spectrum.[35]

Table 2 EPR spin Hamiltonian and strain parameters for $[ReP_2W_{17}O_{62}]^{6-}$ in CH_3CN–C_7H_8 glass[a]

g_x	1.7011(7)	σg_x	−0.011(1)	[+.037]
g_y	1.6646(9)	σg_y	−0.015(1)	[+.044]
g_z	1.8039(9)	σg_z	−0.008(1)	[+.042]
A_x[b]	−1034(2)	σA_x	−8(3)	[+.008]
A_y	−1138(2)	σA_y	−16(3)	[+.014]
A_z	−2104(2)	σA_z	0(3)	[+.000]
θ_{gA}[c]	+15.2°(5)	$\sigma\theta$	−1.1°	[+.072]
P_x[b]	−64.0(5)	σP_x	+1.8(9)	[−.028]
P_y	−75.4(5)	σP_y	−0.1(9)	[+.001]
P_z	+139.4(9)	σP_z	−1.7(9)	[−.012]
θ_{gP}[c]	+10.2°(5)	$\sigma\theta$	−1.1°	

[a] Hyperfine and nuclear quadrupole principal values in MHz (for units of 10^{-4} cm^{-1}, divide by 3). Fractional strain is given in square brackets (for g, $\Delta g(\Delta g)/\Delta g$ is given); correlation parameter of 0.99 used between g, A and P strains. [b] ^{187}Re, $A(^{185}Re) = A(^{187}Re) \times 0.9899$, $P(^{185}Re) = P(^{187}Re) \times 1.05$. [c] Angle of non-coincidence in the yz plane between g and A or P.

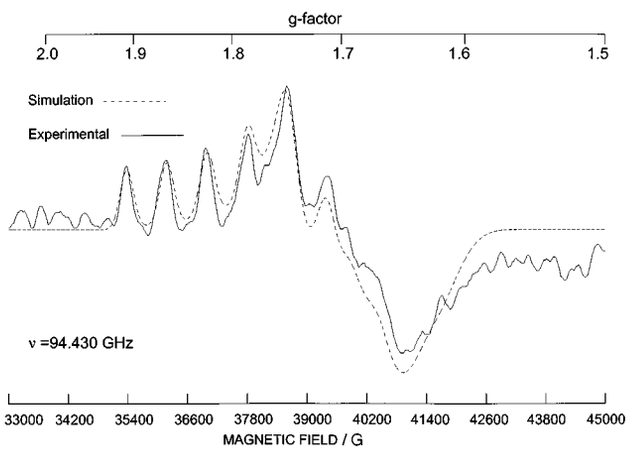

Fig. 7 W-Band (94.43 GHz) electron paramagnetic resonance spectrum of $[\alpha_2\text{-}Re^{VI}OP_2W_{17}O_{61}]^{6-}$ **2** in a CH_3CN/C_7H_8 glass at 20 K. Experimental (——), simulated (– – –).

While the "parallel" portion of the X-band spectrum appears to be first-order, it is not. The peak at highest field, which would be nominally assigned as the parallel feature of the "allowed" $M_I = -5/2$ to $-5/2$ transition, is actually an off-axis extremum peak or angular anomaly. The actual "parallel" $M_I = -5/2$ feature occurs 100 G downfield. Because almost all peaks above 3800 G can be attributed to off-axis peaks in the X-band spectrum and the same above 15000 kG in the Q-band spectrum, the high-field end of these spectra are highly sensitive to non-coincidence between the z-axes of the g-, A- and P-tensors. Non-coincidence of the tensor axes is found only in the yz plane, allowing us to assign the yz plane to the symmetry plane of this C_s system. The non-coincidence is greatest between the g- and A-tensors (15.2°) and smallest between the A- and P-tensors (5.0°), as expected. The axes of the g-tensor are determined primarily by orientations of the ground and excited states, whereas the axes of A are determined by the orientation of the ground state orbital and the axes of P are determined by the orientation of the ligands.[36] By carefully simulating the X-band and Q-band spectra, we can obtain very accurate values of the g, hyperfine, and quadrupole coupling tensors, which are reported in Table 2.

We know of only two other d^1 systems in heteropolytungstates for which values of all three tensors, g, A, and P, were determined.[37,38] The results of all three systems, V(IV), Mo(V), and Re(VI) are reported in Table 3. While for all three systems, the geometry can be described as octahedral with axial and trigonal distortions and with one short terminal oxygen and five shared oxygens, there are expected differences. The structure of the α site in $[PMoW_{11}O_{40}]^{4-}$ should be quite similar to

Table 3 Comparative EPR parameters for d^1 systems in heteropolytungstates[a]

Oxyanion	g_x	g_y	g_z	A_x	A_y	A_z	QD[b]
$[VW_5O_{19}]^{4-}$[c]	1.967	1.967	1.944	176.1	176.1	495.6	−0.29
$[\alpha\text{-}PMoW_{11}O_{40}]^{4-}$[d]	1.9368	1.9340	1.9108	96.5	96.5	221.2	9.0
$[\alpha_2\text{-}P_2ReW_{17}O_{62}]^{6-}$[e]	1.7011	1.6646	1.8039	−1034	−1138	−2104	209.1

[a] Hyperfine and nuclear quadrupole couplings are in units of MHz. Hyperfine couplings are given for V^{51}, Mo^{95} and Re^{187} isotopes. [b] $QD = 3/2\ P_z$; values are given for V^{51}, Mo^{97} and Re^{187} isotopes. [c] Ref. 38. [d] Ref. 37. [e] This work.

the α_2 site in $[\alpha_2\text{-}P_2ReW_{17}O_{62}]^{6-}$ since both have two shared corners and two shared edges, while the vanadium in the $[VW_5O_{19}]^{4-}$ has no shared corners and four shared edges. In addition, the site symmetry is expected to be C_{4v} for the vanadium system, and C_s for the rhenium and molybdenum systems.

Comparison of the g values in Table 3 show two trends. One is the increase in shift from the free-electron g-factor for average value of the g-tensor, *i.e.* the isotropic g-factor, as one goes down the periodic table; the other is the increase in rhombic character and a corresponding decrease in the axial character of the g-tensor. The increase in g-shift is most noticeable between Re and Mo, the ratio of isotropic g-shifts being 3.71. This increase can be readily explained by a large spin–orbit coupling (SOC) for Re, which is expected to be 4.25 times larger than for Mo.[39]

For a system with C_s symmetry, the ground state orbital wavefunction will be hybridized from $d_{x^2-y^2}$, d_{z^2}, d_{yz}, and ligand orbitals, the x axis being normal to the symmetry plane and bisecting the O–Re–O bonds and the z-axis lying approximately along the terminal Re–O bond and normal to the plane of the four in-plane oxygen atoms. This wavefunction can be written as

$$\psi_0 = \alpha(a|x^2 - y^2\rangle + b|z^2\rangle + c|yz\rangle) - \alpha'|L_0\rangle \quad (1)$$

with excited states

$$\psi_1 = \beta\,|xy\rangle - \beta'|L_1\rangle \quad (2)$$

$$\psi_2 = \gamma\,|xz\rangle - \gamma|L_2\rangle \quad (3)$$

$$\psi_3 = \delta(a\,|yz\rangle - c\,|x^2 - y^2\rangle)/\sqrt{a^2 + c^2} - \delta'|L_3\rangle \quad (4)$$

$$\psi_4 = \eta((a^2 + c^2)\,|z^2\rangle - ab\,|x^2 - y^2\rangle - bc\,|yz\rangle)/\sqrt{a^2 + c^2} - \eta'|L_4\rangle \quad (5)$$

where $|L_o\rangle$, $|L_1\rangle$, *etc.* are appropriate symmetry adapted linear combinations of ligand orbitals. Expressions for g and A can be derived for C_s symmetry similarly to those for C_{2v} symmetry.[40] Assuming b and c are much smaller than a and terms in b^2, c^2 and bc are ignored, the resulting equations for g are

$$\Delta g_{zz} = -8a^2\Delta_{xy} \quad (6)$$

$$\Delta g_{yz} = -2ac[2\Delta_{xy} + \Delta_{xz}] \quad (7)$$

$$\Delta g_{yy} = -2a(a - 2\sqrt{3}b)\Delta_{xz} \quad (8)$$

$$\Delta g_x = -2a(a + 2\sqrt{3}b)\Delta_{yz} \quad (9)$$

where $\Delta g_{pq} = g_{pq} - g_e$. To first order, $\Delta_{xy} = \alpha^2\beta^2\ \langle\xi\rangle/\Delta E_{xy}$, $\Delta_{xz} = \alpha^2\gamma^2\langle\xi\rangle/\Delta E_{xz}$, and $\Delta_{yz} = \alpha^2\delta^2\langle\xi\rangle/\Delta E_{yz}$; where ΔE_{pq} are the d–d excitation energies from the ground state to the corresponding d_{pq} state, and the rhenium spin–orbit interaction, $\xi(r)$, varies approximately as Z_{eff}/r^3. Overlap, spin-polarization effects, and contributions from bonding orbitals (hole excitations) can also be lumped into Δ_{xy}, Δ_{xz} and Δ_{yz}. The SOC for the oxygen ligands can be readily neglected, but cannot be neglected for neighboring tungsten atoms.

In order to relate the observed angle of non-coincidence between g_z and A_z, θ_{gA}, to the angle of non-coincidence between g_z and the z-axis of the reference system, θ_g, we need use the corresponding equations for the hyperfine tensor components

$$A_{zz} = -P[(\kappa_0 + 4/7\ a^2)a^2 - \Delta g_{zz} - \frac{1\ (3a - \sqrt{3}b)}{14\ (a + \sqrt{3}b)}\Delta g_x - \frac{1\ (3a + \sqrt{3}b)}{14\ (a - \sqrt{3}b)}\Delta g_{yy}] \quad (10)$$

$$A_{yz} = -P[\tfrac{6}{7}ac a^2 - \Delta g_{yz} + \frac{3}{14}\frac{c}{(a - \sqrt{3}b)}\Delta g_{yy} - \frac{3c}{28a}\Delta g_{zz}] \quad (11)$$

$$A_{yy} = -P[(\kappa_0 - \tfrac{2}{7}a(a + 2\sqrt{3}b))a^2 - \Delta g_{yy} + \frac{1\ (3a - \sqrt{3}b)}{14\ (a + \sqrt{3}b)}\Delta g_x + \frac{\sqrt{3}b}{14\ a}\Delta g_{zz}] \quad (12)$$

$$A_x = -P[(\kappa_0 - \tfrac{2}{7}a(a - 2\sqrt{3}b))a^2 - \Delta g_x + \frac{1\ (3a + \sqrt{3}b)}{14\ (a - \sqrt{3}b)}\Delta g_{yy} - \frac{\sqrt{3}b}{14\ a}\Delta g_{zz}] \quad (13)$$

with overlap and ligand terms neglected, as well as taking the Fermi contact term, κ, as being simply equal to κ_0 times α^2. We assume $\Delta_{xz} = \Delta_{yz}$, which is a good approximation, since the hyperfine and nuclear quadrupole coupling tensors are nearly axial. Using this assumption and $P = 1157$ MHz,[40] we find $b = -0.014$, $c = 0.060$, $\alpha^2 = 0.912$, $\kappa_0 = 0.95$, $\theta_A = -4.6°$, and $\theta_g = 10.6°$. The angle of non-coincidence between g and A for molybdenum in $[PMoW_{11}O_{40}]^{4-}$ was found to be 18°,[37] which, when using $P = -150.7$ MHz[41], gives $b = -0.013$, $c = 0.072$, $\alpha^2 = 0.89$, $\kappa_0 = 0.84$, $\theta_A = -4.4°$, and $\theta_g = -22.3°$. The predicted asymmetry in A, $(A_x - A_y)/(A_z - A_{iso})$, equal to −0.09 for the rhenium system, accounts for about half of the observed asymmetry of −0.15. The remaining difference, −0.06, can be attributed to overlap and ligand contributions to $\langle r^{-3}\rangle$. For the molybdenum system, an asymmetry of −0.04 is expected, although the A-tensor was assumed to be axial. EPR data have been reported for $[PVW_{11}O_{40}]^{5-}$ [38] and $[P_2VW_{17}O_{62}]^{7-}$ [42] but the spectra were interpreted assuming C_{4v} symmetry.

The hybridization coefficients, b and c, are small for both rhenium and molybdenum systems, showing that the ground-state wavefunction is primarily $d_{x^2-y^2}$ ($a = 0.99$). The values of c, 0.060 and 0.072, correspond to a tilting of the ground-state $d_{x^2-y^2}$ orbital from the xy plane by −3.4° and −4.2°. While the z axis of the hyperfine tensor is orientated very close to the normal of this tilted $d_{x^2-y^2}$ orbital, that of the g-tensor is not. Also, the tilt in the g-tensor z-axis for the rhenium system is opposite in direction to that for the molybdenum system. The angle of non-coincidence can be related to the elements of g

$$\tan(2\theta_g) = \frac{2\Delta g_{yz}}{\Delta g_{yy} - \Delta g_{zz}} \geqslant -3\ ac\ \frac{\Delta g_{iso}}{\Delta g_{yy} - \Delta g_{zz}} \quad (14)$$

and shows the sensitivity of θ_g to the difference between Δg_{yy} and Δg_{zz}. If Δg_{yy} is very close to Δg_{zz}, θ_g can switch from +45° to −45°. On the other hand, if $(\Delta_{xz} + \Delta_{yz})/2$ is close to Δ_{xy}, Δg_{zz} will be about eight times Δg_{yy}, and the z-axes of the g- and A-tensors will be nearly coincident and aligned with the normal to the tilted $d_{x^2-y^2}$ orbital.

In the rhenium system, the ratio of $(\Delta_{xz} + \Delta_{yz})/2$ to Δ_{xy} is six, while in the molybdenum system it is three and in the vanadium system it is two and a half. The decrease in axial character in the g-tensor as one goes down Table 3, can be explained in terms of an increase in in-plane σ-bonding and a weakening of the axial or terminal M=O bond. With the increase in in-plane metal–ligand covalency, there will be a decrease in the MO coefficient, β, a decrease in $\langle\xi\rangle$ due to increased electron screening (the two-electron part of SOC), an increase in overlap, and added contributions from bonding orbitals, all of which will contribute to the quenching of the in-plane angular momentum and to a decrease in Δ_{xy}. This effect is strong enough for the rhenium system to make Δg_z smaller than Δg_x and Δg_y.

The nuclear quadrupole tensor represents the total electric field gradients at the metal nucleus and includes contributions from the paired bonding electrons as well as that from the unpaired electron. The principal nuclear quadrupole coupling constant can be expressed as

$$\frac{4I(2I-1)}{3}QD = e^2Qa^2q_{5d}(1-R) + e^2Qq_{ov}(1-R) + e^2Qq_{lig}(1-\gamma)$$

where q_{5d} is equal to $\langle r^{-3}\rangle_d$, q_{ov} and q_{lig} are the overlap and ligand contributions to $\langle r^{-3}\rangle$, and R and γ are the Sternheimer shielding and antishielding constants. The first term is determined primarily by the unpaired electron density, giving a similar contribution to the hyperfine tensor, while the third term is dominated by contributions from the paired electron density and surrounding nuclear charges. While the third term is equal to zero for octahedral geometry, it is very sensitive to deviations from octahedral symmetry. Rhenium is expected to have a large value of QD ($3/2\ P_z$), since QD scales as the product of nuclear quadrupole moment and $\langle 1/r^3\rangle$. $Q(Re^{187}/Mo^{97})$ is equal to 11.1 and the average value of $1/r^3$ is 2.19 times larger for rhenium than molybdenum.[41] Assuming the ligand fields are similar and neglecting differences in effective charge and relativistic effects, one expects that the value of QD should be 24.2 times larger for the rhenium system than for the molybdenum system (Table 3). This value compares extremely well to the observed ratio of 23.4 : 1. The corresponding scaling factor between V^{51} and Mo^{97} is expected to be −11.3 : 1, although a larger ratio, −31.5 : 1, is actually observed between the vanadium and molybdenum systems. The poor scaling between the vanadium and molybdenum systems can be in part attributed to the difference in structure between the vanadium system and that of the molybdenum and rhenium systems, but also to smaller in-plane metal–ligand covalency expected for vanadium. These differences show up more in the nuclear quadrupole coupling than the hyperfine interaction, because of nuclear quadrupole coupling's sensitivity to geometric changes in the ligand field.

The angle of non-coincidence between the z-axes of the A-tensor and the rhenium nuclear quadrupole coupling tensor is found to be 5.0°, and corresponds to a tilt of 0.4° from the z-axis of the nuclear quadrupole tensor from the reference z-axis. If only the first term in the above equation is considered and the contribution from bonding valence electrons neglected, this angle would be −3.5°, the same as the tilt angle of the hybrid d orbital. The alignment of the nuclear quadrupole tensor by the ligand geometry rather than the ground-state orbital is due to the importance of the ligand field contributions. The asymmetry parameter, $(P_x - P_y)/P_z$, expected for our hybrid d orbital, will be equal to −0.04, but instead, a value of +0.08 is observed. The ligand field will polarize the d electrons producing electric field gradients that oppose those of the ligands. Because the quadrupole coupling is much more sensitive to the ligand field gradient than is the hyperfine tensor, the asymmetry parameter for the hyperfine will be reversed from that of the nuclear quadrupole coupling.

The EPR linewidth of the rhenium center in $[ReOP_2W_{17}O_{61}]^{6-}$ is dominated by a highly correlated g-strain, The strain in the three principal values of g, A, and P were assumed then to be totally correlated; that is, $\varepsilon = \pm 1$. The overall strain due to g, ΔW_g, A, ΔW_A, and P, ΔW_P, is then convoluted to give the net Gaussian linewidth, ΔW:

$$\Delta W^2 = \Delta W_r^2 + \Delta W_g^2 + \Delta W_A^2 + \Delta W_P^2 + 2(\varepsilon_{gA}\Delta W_g\Delta W_A + \varepsilon_{gP}\Delta W_g\Delta W_P + \varepsilon_{AP}\Delta W_A\Delta W_P)$$

where, ΔW, is the residual or intrinsic linewidth, which was found to have an isotropic value of 22.5 G, and ε_{gA} is the correlation between g and A strains, *etc*. The g-strain along all three axes is roughly proportional [$\Delta(\Delta g)/\Delta g$ ranges from +0.037 to +0.044] to the shift from the free electron g-factor, $g_e = 2.00236$. An increase in Δg corresponds to an increase in Δ_{xy}, Δ_{xz} and Δ_{yz} and an increase in unquenched angular momentum due to a decrease in the ligand field.

A highly correlated strain is also found for the hyperfine tensor, $\varepsilon_{ga} = 0.99$, but is both relatively smaller and quite anisotropic as compared to the strain in g. This is the opposite of the behavior seen for copper d^9 systems, where the A-strain is proportionally larger than the g-strain.[43] The small A-strain for rhenium can be explained by differentiating eqn. (10)–(13) with $b = -0.014$, $c = 0.060$, $\alpha^2 = 0.912$ and $\kappa_0 = 0.95$.

$$\Delta A_{zz} = -P\,[0.74\Delta a - \Delta(\Delta g_{zz}) - 0.22\Delta(\Delta g_x) - 0.21\Delta(\Delta g_{yy}) + 0.08\Delta b] \quad (15)$$

$$\Delta A_{yz} = -P\,[0.02\Delta a - \Delta(\Delta g_{yz}) + 0.01\Delta(\Delta g_{yy}) - 0.01\Delta(\Delta g_{zz}) - 8.04\Delta c] \quad (16)$$

$$\Delta A_{yy} = -P\,[0.35\Delta a - \Delta(\Delta g_{yy}) + 0.22\Delta(\Delta g_x) - 0.00\Delta(\Delta g_{zz}) - 0.89\Delta b] \quad (17)$$

$$\Delta A_x = -P\,[0.34\Delta a - \Delta(\Delta g_x) + 0.21\Delta(\Delta g_{yy}) + 0.00\Delta(\Delta g_{zz}) + 0.89\Delta b] \quad (18)$$

If Δa is small, the strain in A will be dominated by the strain in g and changes in hybridization. The A-strain in d^1 systems is expected to be much smaller than in d^9 systems, because Δg for d^1 systems is opposite in sign from that in d^9 systems where it adds in phase to the Δa term. The changes in hybridization, as determined from the g-strain, and the correlated part of the angular strain non-coincidence between g and A (−0.88°, $\varepsilon = 0.81$), are $\Delta b = -0.0011$, $\Delta c = -0.0048$. While these changes are small, they make a large impact on the A-strain, in particular in the off-diagonal element. Using $P = 1157$ MHz and $\Delta a = -0.01$ gives $\Delta A_{zz} = -6.5$ MHz, $\Delta A_{yy} = -9.4$ MHz, $\Delta A_x = -4.1$ MHz, and a very large $\Delta A_{yz} = 42.7$ MHz. In the frame in which A is diagonal these values become $\Delta A_z = +0.4$ MHz, $\Delta A_y = -16.3$ MHz, and $\Delta A_x = -4.1$ MHz, which compare very well to the observed values of 0, −16 and −8, respectively.

The strain in the components of the nuclear quadrupole coupling tensor is also correlated ($\varepsilon_{gP} = 0.95$) to the A-strain but in an opposite phase. Along y, the strain is largest in A and yet smallest in P. While P and the anisotropic part of A are both measures of the electric field gradient at the nucleus, the nuclear quadrupole tensor does not include contributions from the g-tensor. Considering only the dipolar contributions in the above equations for the hyperfine coupling and using $\Delta a = -0.01$, gives $\Delta P_z = -0.9$ MHz, $\Delta P_y = +0.8$ MHz, and $\Delta P_x = +0.1$

MHz. The strain along z is underpredicted, but we have included only the unpaired electron contribution to P. The strains along x and y are reversed. However, it has been noted that the equilibrium asymmetry parameter of the P-tensor (+0.08) is opposite in direction from that of the A-tensor (−0.15) so that for both P and A, an increase in the magnitude of asymmetry along with a corresponding increase in $\Delta b/b$ and a decrease in $\Delta c/c$ is correlated with the increase in Δg.

In addition, to the strain-induced variation in the angle of non-coincidence between g and A in the yz plane of −1.1°, an angular deviation of 2.5° of the z-axis of the g-tensor away from that of the yz plane was needed to simulate the EPR spectra. Unlike the in-plane angular variation, which is well correlated to the other strain parameters ($\varepsilon = 0.81$), the out-of-plane variation is not and is the only strain for which the planar symmetry is broken. Thus, there are probably two different types of strains, one in which the rhenium and terminal oxygen are pulled away from the polyoxoanion framework and another in which the rhenium and terminal oxygen are bent out of the plane of symmetry. In the former, additional stretching of the Re=O bond would be needed to give an increase in the g-shift along all three directions. Along with the increase in g-shifts is a decrease in $\Delta c/c$, an increase in $\Delta b/b$, and a decrease in $\Delta QD/QD$. The increase in $\Delta b/b$ corresponds to an increase in rhombic character, which is opposite to what would be predicted from our model and probably results from increased directed solvent interaction with the Re=O group.

The X-band and Q-band spectra reported for $[RePW_{11}O_{40}]^{5-}$ and $[ReSiW_{11}O_{40}]^{6-}$ are qualitatively similar to the rhenium spectra reported in this paper.[10] However, the earlier analyses did not include the effects of the rather large nuclear quadrupole coupling or take into account the possible non-coincidence between the tensors and thus, it is difficult to quantitatively compare the EPR parameters.[44]

Conclusion

We have prepared $K_7[\alpha_2\text{-}Re^{V}OP_2W_{17}O_{61}]$ by reaction of $Re^{IV}Cl_6^{2-}$ with the $[\alpha_2\text{-}P_2W_{17}O_{61}]^{10-}$ isomer, following the example of Charreton and Meunier. This complex was characterized using electrospray mass spectrometry and multinuclear NMR techniques among other techniques. Cyclic voltammetry in aqueous solution shows four non-reversible oxidation–reduction processes. Multiple charge states as well as varying amounts of cation adducts to the multiply charged clusters are observed in the negatively charged electrospray mass spectrometry. ^{183}W NMR spectroscopy confirms the C_s symmetry of the molecule. The NBu_4^+ analog of this complex, $[NBu_4]_xK_{7-x}[\alpha_2\text{-}Re^{V}OP_2W_{17}O_{61}]$, is extremely air sensitive oxidizing to the Re^{VI} analog upon exposure to air. The Re^{VI} analog, $[NBu_4]_6[\alpha_2\text{-}Re^{VI}OP_2W_{17}O_{61}]$, can be prepared simply by metathesis of the Re^{V} material with tetrabutylammonium ion in air. The ^{31}P NMR, EPR and mass spectral data are consistent with a paramagnetic Re^{VI} species. Cyclic voltammetry of an acetonitrile solution of the Re^{VI} species shows four reversible redox features. The X-band, Q-band and W-band EPR spectra of **2** show extreme variations in linewidths due to random strains or distortions of the complex. Simulations of the X-band and Q-band EPR spectra allow determination of the g, hyperfine and quadrupole coupling tensors; the molecule has rhombic character due to an increase in in-plane σ bonding and a weakening of the axial M=O bond. $[NBu_4]_6[\alpha_2\text{-}Re^{VI}OP_2W_{17}O_{61}]$ can be oxidized by AgO_3SCF_3 to give the Re(VII) analog, **3**.

Acknowledgements

We acknowledge the following sources of support for this research: Faculty Research Award Program of the City University of New York, Eugene Lang Faculty Development Award, NSF-CHE9309001, NSF-CHE9502213 (L. C. F.), NIH-Research Centers in Minority Institutions Grant RR03037-08S2, and NSF Grant PCM8111745 for the purchase of the 400 MHz Spectrometer. NIH Research Resources Grant P-41-RR01811 is acknowledged for the use of IERC resources.

References

1 M. T. Pope, *Heteropoly and Isopoly Oxometalates*, Springer, New York, 1983; M. T. Pope and A. Muller, *Angew. Chem., Int. Ed. Engl.*, 1991, **30**, 34.
2 D. C. Crans, *Comments Inorg. Chem.*, 1994, **16**, 35 and refs. therein; D. C. Crans, *Polyoxometalates: From Platonic Solids to Anti-Retroviral Activity*, eds. A. Muller and M. T. Pope, Kluwer Academic Publishers, The Netherlands, 1993, pp. 399–406; C. L. Hill, M. S. Weeks and R. F. Schinazi, *J. Med. Chem.*, 1990, **33**, 2767; M. S. Weeks, C. L. Hill and R. F. Schinazi, *J. Med. Chem.*, 1992, **35**, 1216 and refs. therein; G.-S. Kim, D. A. Judd, C. L. Hill and R. F. Schinazi, *J. Med. Chem.*, 1994, **37**, 816; N. Yamamoto, D. Schols, E. deClercq, Z. Debyser, R. Pauwels, J. Balzarini, H. Nakashima, M. Baba, M. Hosoya, R. Snoeck, J. Neyts, G. Andrei, B. A. Murrer, B. Theobald, G. Bossard, G. Henson, M. Abrams and D. Picker, *Mol. Pharmacol.*, 1992, **42**, 1109; Y. Inouye, Y. Tokutake, T. Yoshida, Y. Seto, H. Hujita, K. Dan, A. Yamamoto, S. Nishiya, T. Yamase and S. Nakamura, *Antiviral Res.*, 1993, **20**, 317; D. A. Judd, R. F. Schinazi and C. L. Hill, *Antiviral Chem. Chemother.*, 1994, **5**, 410.
3 For recent reviews, see C. L. Hill and C. M. Prosser-McCartha, *Coord. Chem. Rev.*, 1995, **143**, 407 and refs. therein; N. Mizuno and M. Misono, *J. Mol. Catal.*, 1994, **86**, 319; I. V. Kozhevnikov, *Chem. Rev.*, 1998, **98**, 171; N. Mizuno and M. Misono, *Chem. Rev.*, 1998, **98**, 199; M. Sadakane and E. Steckhan, *Chem. Rev.*, 1998, **98**, 219.
4 R. Neumann and M. Dahan, *J. Chem. Soc., Chem. Commun.*, 1995, 1995; C. L. Hill and R. B. Brown, Jr., *J. Am. Chem. Soc.*, 1986, **108**, 536; R. Neumann and M. Dahan, *Nature* (*London*), 1997, **388**, 353.
5 D. Mansuy, J.-F. Bartoli, P. Battioni, D. K. Lyon and R. G. Finke, *J. Am. Chem. Soc.*, 1991, **113**, 7222.
6 J. Bartis, S. Sukal, E. Kraft, R. Kronzon, M. Dankova, M. Blumenstein and L. C. Francesconi, *J. Chem. Soc., Dalton Trans.*, 1997, 1937; Q.-H. Luo, J. Bartis, M. Dankova, N. Ullah, V. Young and L. C. Francesconi, manuscript in preparation.
7 J. Bartis, M. Dankova, M. Blumenstein and L. C. Francesconi, *J. Alloys Comp.*, 1997, **249**, 56.
8 A. Venturelli and L. C. Francesconi, American Chemical Society Meeting, San Francisco, April, 1997.
9 E. Deutsch, K. Libson and J.-L. Vanderheyden, in *Technetium and Rhenium in Chemistry and Nuclear Medicine*, eds. M. Nicolini, G. Bandoli and U. Mazzi, Cortina International, Verona Raven Press, New York, 1990. In some situations, Re is a suitable replacement for Tc. This is seen in the vast literature on Tc and Re small coordination complexes. However, the kinetic inertness of Re compared to Tc as well as the higher reduction potentials of Re compared to Tc may result in very different behavior of the two elements in some matrices such as metal oxides.
10 F. Ortéga and M. T. Pope, *Inorg. Chem.*, 1984, **23**, 3292.
11 F. Ortéga, M. T. Pope and H. T. Evans, *Inorg. Chem.*, 1997, **36**, 2166.
12 B. Charreton and R. C. R. Meunier, *C.R. Hebd. Seances Acad. Sci., Ser. C*, 1974, **275**, 945.
13 T. L. Jorris, M. Kozik, N. Casan-Pastr, P. J. Domaille, R. G. Finke, W. K. Miller and L. C. W. Baker, *J. Am. Chem. Soc.*, 1987, **109**, 7402.
14 D. K. Lyon, W. K. Miller, T. Novet, P. J. Domaille, E. Evitt, D. C. Johnson and R. G. Finke, *J. Am. Chem. Soc.*, 1991, **113**, 7209.
15 M. Kozik, R. Acerete, C. F. Hammer and L. C. W. Baker, *Inorg. Chem.*, 1991, **30**, 4429.
16 K. P. Gable, *Adv. Organomet. Chem.*, 1997, **41**, 127.
17 W. A. Herrmann and F. E. Kuhn, *Acc. Chem. Res.* 1997, **30**, 169.
18 W. A. Herrman, *Angew. Chem., Int. Ed. Engl.*, 1988, **27**, 1297.
19 A. M. Al-Ajlouni and J. H. Espenson, *J. Am. Chem. Soc.*, 1995, **117**, 9243.
20 A. K. Yudin and K. B. Sharpless, *J. Am. Chem. Soc.*, 1997, **119**, 11536.
21 W. J. Randall, M. W. Droege, N. Mizuna, K. Nomiya, T. J. R. Weakley and R. G. Finke, *Inorg. Synth.*, 1997, 167.
22 R. B. Clarkson, W. Wang, M. J. Nilges and R. L. Belford, *Influence of Organic Sulfur in Very High Frequency EPR of Coal,* in *Processing and Utilization of High-Sulfur Coal*, eds. R. Markuszewski and T. D. Wheelock, Elsevier, Amsterdam, 1990, pp. 67–77.
23 M. J. Nilges, SIMPIP, Illinois EPR Center, University of Illinois, 1998.

24 M. J. Nilges, PhD Thesis, University of Illinois, Urbana-Champaign, 1979.
25 K. Mattson, PhD Thesis, University of Illinois, Urbana-Champaign, 1991.
26 W. J. Randall, T. J. R. Weakley and R. G. Finke, *Inorg. Chem.*, 1993, **32**, 1068.
27 M. R. Antonio, L. Soderholm, G. Jennings, L. C. Francesconi, M. Dankova and J. Bartis, *J. Alloys Compds.*, 1998, **275–277**, 827.
28 N. Haraguchi, Y. Okaue, T. Isobe and Y. Matsuda, *Inorg. Chem.*, 1994, **33**, 1015.
29 D. A. Malikov, M. S. Milyukova, E. V. Kuzovkina and B. F. Myasoedov, *Sov. Radiochem.* (*Engl. Transl.*), 1992, **34**, 106; A. S. Saprykin, V. P. Shilov, V. I. Spitsyn and N. N. Krot, *Dokl. Akad. Nauk SSSR*, 1976, **226**, 853.
30 R. Massart, R. Contant, J.-M. Fruchart, J.-P. Ciabrini and M. Fournier, *Inorg. Chem.*, 1977, **16**, 2916.
31 L. C. Francesconi, G. Graczyk, S. Wehrli, S. N. Shaikh, D. McClinton, S. Liu, J. Zubieta and H. F. Kung, *Inorg. Chem.*, 1993, **32**, 3114; C. S. John, L. C. Francesconi, S. Wehrli, G. Grazyck, P. A. Carroll and H. F. Kung, *Polyhedron*, 1992, **11**, 1145; S. Sukal, J. E. Bradshaw, J. He, G. P. A. Yap, A. Rheingold, H. F. Kung and L. C. Francesconi, *Polyhedron*, 1998, in the press.
32 M. J. Abrams, C. E. Costello, S. N. Shaikh and J. Zubieta, *Inorg. Chim. Acta.*, 1991, **180**, 9.
33 *Electrospray Ionization Mass Spectrometry*, *Fundamentals Instrumentation and Applications*, ed. Richard B. Cole, John Wiley and Sons, New York, 1997.
34 (*a*) T.-C. Lau, J. Wang, R. Guevremont and K. W. M. Siu, *J. Chem. Soc.*, *Chem. Commun.*, 1995, 877; (*b*) M. J. Deery, O. W. Howarth and K. R. Jennings, *J. Chem Soc.*, *Dalton Trans.*, 1997, 4783.
35 K. S. Rothenberger, M. J. Nilges, T. E. Altman, K. Glab, W. Froncisz and J. S. Hyde, *Chem. Phys. Lett.*, 1986, **124**, 295.
36 M. J. Nilges and R. L. Belford, *J. Magn. Reson.*, 1979, **35**, 259.
37 G. D. Simpson, PhD Thesis, University of Illinois, Urbana-Champaign, 1978.
38 D. P. Smith, H. So, J. Bender and M. T. Pope, *Inorg. Chem.*, 1973, **12**, 685.
39 J. Bendix, M. Brorson and C. E. Schäffer, *Inorg. Chem.*, 1993, **32**, 2838.
40 B. R. McGarvey, *Transition Met. Chem.*, 1966, **3**, 89.
41 J. R. Morton and K. F. Preston, *J. Magn. Reson.*, 1978, **30**, 577.
42 S. P. Harmalker, M. A. Leparulo and M. T. Pope, *J. Am. Chem. Soc.*, 1983, **105**, 4286.
43 W. Froncisz and J. S. Hyde, *J. Chem. Phys.*, 1980, **73**, 3123.
44 For $[RePW_{11}O_{40}]^{5-}$ and $[ReSiW_{11}O_{40}]^{6-}$, markedly rhombic hyperfine tensors were reported.[10] We have found that this results when the non-coincidence between the g and A tensors is neglected. These systems, like the molybdenum and rhenium systems reported here, should have marked non-coincidence between g and A in the xz plane (yz plane according to our coordinate definition) and nearly axial A-tensors.

Paper 8/05286C